FEASIBILITY ASSESSMENT OF A FINE GUIDANCE SENSOR IN THE INFRARED BAND

Andrea Bosco [(1)], Nicolas Deslaef [(2)], Alessandro Spagna [(3)]

[(1)] Thales Alenia Space Italy, Strada Antica di Collegno 253,10146 Torino, Italy, +39 01119787859, andrea.bosco@thalesaleniaspace.com

[(2)] ESA/ESTEC, Keplerlaan1, Postbus 299, 2200 AG Noordwijk, The Netherlands, +31 71565 4721, Nicolas.Deslaef@esa.int

[(3)] INAF Astrophysical Observatory of Turin, Via Osservatorio 20, 10025 Pino Torinese, +39 0118101983, alessandro.spagna@inaf.it

ABSTRACT

The Fine Guidance Sensor (FGS) aims at refining the pointing accuracy of a payload up to 2 orders of magnitude better than standard AOCS equipment. The FGS cannot be considered as "standard equipment", being especially tailored and designed under the main constraints of the scientific requirements of a specific mission. For the ESA M5 candidate SPICA mission, requiring an unprecedented attitude estimation performance for an infrared mission, Thales Alenia Space Italy (TAS-I) performed in 2020 a first assessment of feasibility for an FGS in the infrared band by exploring the architecture, the available detectors and the infrared star catalogues with the support of INAF Astrophysical Observatory of Turin. During this assessment the following activities were successfully completed: trade-offs and sensitivity analyses on the FGS design with the detector selection and its accommodation, the sensitivity analysis on the size of the FOV, the sensitivity of the performance in terms of sky coverage and FGS Attitude Knowledge Error (AKE) to the integration time, while considering all the design constraints in terms of environment, operations and accommodation.

1 THE FINE GUIDANCE SENSOR

1.1 General FGS configuration

In general terms the Fine Guidance Sensor (FGS) is an instrument that allows refining the pointing accuracy of a payload, in relative and/or absolute terms, up to 2 orders of magnitude better than standard AOCS equipment to guarantee the most recent platform performances that becomes more and more demanding. The FGS can be required either to compute with high accuracy relative rotations occurred during a scientific survey minimizing the pointing jitter or to compute the absolute attitude with respect to the inertial frame: the design impacts are rather different depending on the cases. In the first case, the FGS must "simply" lock some initial target and determine the evolution of these targets on the focal plane allowing for relative rotations calculation (or delta quaternion). In the second case, a star catalogue is needed on board to allow absolute quaternion computation. This can be an operative demanding task as a continuous update of the catalogues (generation and transmission to S/C) may be needed. Beyond these pointing needs, the FGS can also be in charge of collecting sky images that could be used to support the scientific objectives of the mission or for troubleshooting/calibration purposes.

The FGS configuration can largely vary over different spacecraft as different accommodations with other payload instruments, environmental conditions and required functionalities are defined in different missions. The FGS architecture largely affects the development strategy, the responsibility (science consortium or industry) and the verification plans. In general terms the FGS is composed by the following assemblies:

- Optical assembly (Telescope, Instrument optical channel)
- Detectors, on the FGS focal plane assembly (FPA)
- Readout electronics (based on FPGA/ASIC technologies)
- Instrument electronic units (power distribution and data processing)

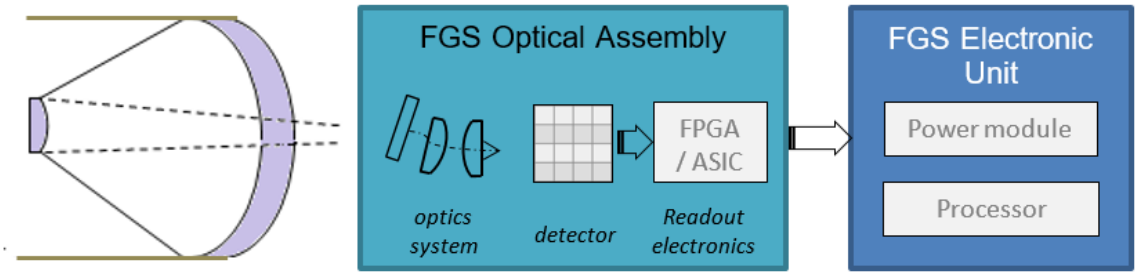

Figure 1. Fine Guidance Sensor generic configuration

The Focal Plane Assembly is a very peculiar item since of the thermal aspects (including thermal loads produced on surrounding equipment's), alignments and stabilities issues. The presence of a dedicated optics for the FGS is an aspect that can discriminate design characteristics and complexity of the FGS:

- In case the FGS is based on the main telescope optics, many trade off and architectural solutions are fixed at spacecraft level: the optics characteristics and focal plane constraints (thermal conditions, mechanical I/F and assembly flow) are inherited by the FGS design from the S/C design, and the other design solutions are aimed to cope with these conditions;
- In case the FGS is considered as a stand-alone unit with its own optics, a larger flexibility in the design is achieved, as all the system parameters can be selected on the basis of the FGS needs.

As general consideration, the former will allow using a large telescope with long focal length, while the latter will allow for use of reduced size telescope with shorter focal length. The decision of using an FGS based on the main telescope requires significant design integration between spacecraft responsible and FGS responsible since the early phase of the system study.
In addition, it must be noted that EMC issues are in general more critical in case of an FGS sharing optics with the telescope. In fact, in this case the FPA and FEE must be put in close vicinity to other focal planes of the instruments placed on the telescope focal plane. This noise, if not reduced, would be the dominant in the FGS noise budget. Even worse, the same level of noise could be injected by the FGS to the main instrument, completely jeopardizing its functionality.

While the Optics and the FPA are usually accommodated in the Payload module, the electronic unit is typically well separated; in fact, the FGS is a high demanding computational capability system requiring significant power consumption and large dimensions that makes unfeasible the accommodation close to the focal plane. The Application SW processing the acquired star data to derive the attitude can be hosted in the same Electronic Unit or into the central computer depending

on the selected architecture. The way the different assemblies can be grouped together is in some way dependent on spacecraft needs. The Electronic Unit can be a separated unit where power conditioning and CPU functions are allocated, or can be responsible only for power conditioning. The unit can have two channels redounded for reliability reasons. The number of detectors and processing electronics channels to be used for attitude measurement can vary, depending on system accommodation and needs as well. The optimal cross strapping philosophy is that each readout channel is connected to all the detector and to the Electronic Unit independently.

2 SPICA MISSION CASE AND FGS TRADE-OFF

SPICA (Space Infrared Telescope for Cosmology and Astrophysics), a mission still in its study phase, would have been, if selected, a joint European-Japanese program. An ambitious technological concept featuring a cryogenically cooled telescope, SPICA aimed to greatly improve on the sensitivity of previous infrared space observatories, and to study a wide range of scientific topics, such as the formation of stars, planets and galaxies. SPICA was one of three candidate missions for the selection of the 5th medium-sized mission (M5) of ESA's Cosmic Vision Programme as its current long-term planning framework of space science missions. In October 2020, ESA and JAXA announced that SPICA was removed from the M5 selection due to the strict financial constraints faced by both agencies, and the satellite system design studies were concluded soon after.

SPICA is designed to observe mid- to far-IR wavelengths between 12-230μm, with very high sensitivity. Using a primary mirror actively cooled to < 8K, SPICA can expect to achieve a gain in sensitivity of more than two orders of magnitude over both Spitzer and Herschel in the mid and far-IR. In order to determinate and control the Observatory attitude with the accuracy requested by the science operations, the SPICA AOCS subsystem shall implement a Fine Guidance Sensor able to provide very accurate estimation of the Observatory absolute attitude, in the order of sub-arcsecond. The optical assembly is requested to be compatible with the cryogenic environment where the operative temperature is close to 4.8K and the detector is requested to dissipate less than 1mW. This would require an ad-hoc qualification of the detectors and readout electronics. An alternative has been assessed with possibility to operate into a warmer separate environment with temperature around 30K with a slightly relaxed detector power dissipation of 5mW. However, this accommodation has been discarded because the higher power dissipation would affect the PLM thermal environment. The environment in which the FGS optical assembly is placed imposes important constraints on the selection of the IR detector and the components to be mounted on the readout electronics boards, that shall be compatible with the severe thermal operative conditions.
The other challenging aspect for the FGS design, is the requested Attitude Knowledge Error (AKE) performance, that is apportioned into bias contribution, which shall be lower than 0.1 arcsec and 92 arcsec @99.7% confidence level respectively across and around Line of Sight, and a time dependent part, which shall be lower than 0.01 arcsec and 9.2 arcsec @99.7% confidence level across and around Line of Sight. Such performance shall be achieved in low rate condition, i.e. with an angular velocity that is lower than 0.15 arcsec/s as specified by requirement. The characterization of the performance in high rate has been requested, determining the maximum tolerated angular rate for attitude measurement.

The study performed by Thales Alenia Space Italy aimed to demonstrate the feasibility of the SPICA FGS design based uniquely on technologies, which are projected to achieve at least Technology Readiness Level (TRL) of 6 by the time of the mission adoption that should have been 2024. This was achieved by performing several trade-offs on detector selection and its

accommodation, with sensitivity analysis of the performance (Sky coverage and FGS Attitude Knowledge Error (AKE)) to the integration time and Field of View.

2.1 FGS Trade-offs result

The first important trade-off is on the detector selection that drives the compatibility with the environment, the readout frequency and the availability of IR star catalogue. The IR detectors available for the Near, Mid and Far IR can be divided into two main categories:

- NIR (near-infrared) detectors. They are hybrid CMOS silicon detectors based on HgCdTe substrate plus a readout integrated circuit. These are the most widely used detector for Near IR since HgCdTe material provides near-theoretical performance and can be fabricated at different cut-off wavelength (from 1.5μm and 5μm) varying the Hg-to-Cd ratio. The Hawaii detector family of the U.S. Teledyne company [2], are the most widespread and proven solution; it can be available in format 2048x2048 pixels (H2RG with 18μm pitch) and 4096x4096 pixels (H4RG with 10μm pitch under development) and the SIDECAR ASIC can be provided together with the detector performing all functionality required for focal plane electronics. The Sofradir company is developing an European detector named ALFA [3] with characteristics similar to Hawaii in terms of sensitive band, quantum efficiency and readout frequency. It has reached recently TRL 4 level.

- Mid-Far IR detectors. They are Impurity Band Conduction (IBC) or Blocking Impurity Band (BIB) detectors based on Si:As or Si:Sb blocking material plus a readout integrated circuit. These type of detectors are more dedicated to longer wavelengths up to 30-40μm. Raytheon Vision System produced Si:As detector for ground (ESO) and space application (MIRI instrument of JWST [4][5]) with 1024x1024 pixel format. Unfortunately it has been understood that the production for the space application would be interrupted after MIRI. The DRS U.S. company has developed some Si:As and Si:Sb for Spitzer and WISE missions [6] and is the candidate for providing the detector of SPICA SMI instrument [7],[8] and [9]. The format is 1024x1024pixels, with 18μm pitch, but the current status of qualification is not well known.

The NIR detector shows a higher quantum efficiency around 1-3μm wavelength, while Mid-Far IR detector shows a lower efficiency but over wider band (Figure 2). Because of the technologies, the two categories are suitable to different environment: HgCdTe can be operated into cold environment at temperature between 30K and 100K with power dissipation around 3mW at slow readout, which increase significantly at higher readout speed; Si:As and Si:Sb can be operated into cryogenic environment below 10K and provide a very small dissipation (0.5mW per output). For both technologies the level of dark current (<1el/sec/pix) is negligible for FGS application. The readout noise of NIR detector (10 - 25 electrons rms depending on the detector) is a bit better than Mid-Far IR ones (40 and 100 electrons rms for Si:As and Si:Sb respectively).

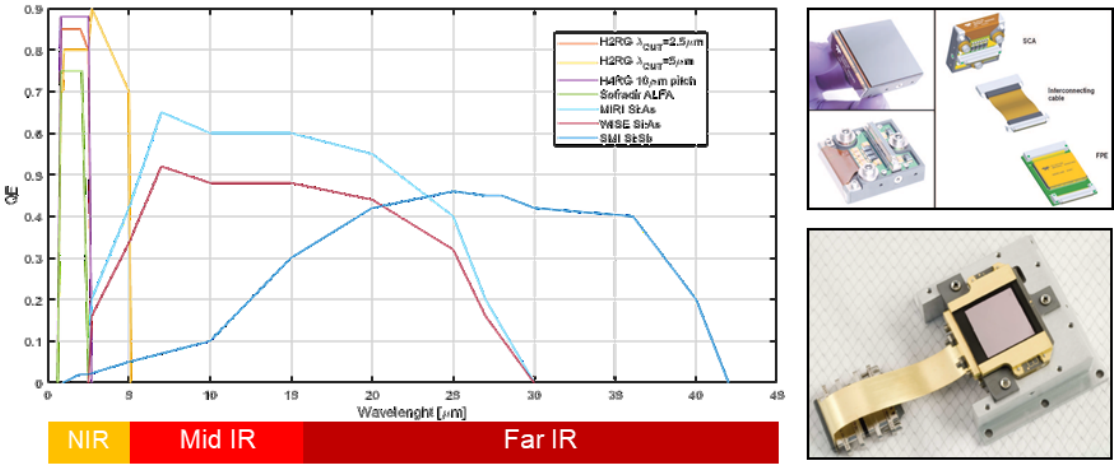

Figure 2. IR detector QE (left). MIRI detector top

All these characteristics translate into Signal-to-Noise Ratio (SNR) which is significantly better for NIR detector with detection of stars up to 19th-20th magnitude considering SPICA telescope design and 1s of exposure time. The Mid-Far IR detectors are sensible up to 14th-15th magnitude for same assumptions. The maximum detectable magnitude however is not an absolute criterion, since for inertial attitude measurement, a star catalogue is needed, and the detectable star magnitude limit shall be compared with the magnitudes of stars reported in the astrometric catalogues for different wavelength. For this reason, it has been examined the current available IR star catalogues covering the entire sky.

Table 1: All sky surveys in the optical and IR passband

Catalogue	Passband	Epoch	Object Number	Position Accuracy
Gaia DR2	G, GBP, GRP (~0.65, 0.5, 0.8 μm)	2015.5	1 692 919 135	0.04 mas (G<14) → 0.7 mas (G=20)
Gaia DR3	G, G BP , G RP (~0.65, 0.5, 0.8 μm)	2016	1 811 709 771	0.01 mas (G<15) → 0.4 mas (G=20)
2MASS	J, H, Ks (1.25, 1.65, 2.18 μm)	1997 - 2001	470 992 970	200 mas (J<10) → 500 mas (J=17)
CatWISE	W1, W2 (3.3, 4.7 μm)	2015.2	1 890 715 640	50 mas (W1<12) → 270 mas (W1=18)
AllWISE	W1, W2, W3, W4 (3.3, 4.7, 12, 22 μm)	2010.25	747 634 026	150 mas (W3<10) → 500 mas (W3<14)

The state of the art in terms of star catalogue is absolutely Gaia catalogue, thanks to the sub-milli-arcsecond astrometric accuracy and the availability of the five-parameter astrometric solution (positions on the sky (α, δ), parallaxes, and proper motions) for about 1.5 billion of sources over the entire sky. The most updated release of the mission at the beginning of the study (2020) was the Gaia second data release (Gaia DR2), afterwards updated by the early third data release (Gaia EDR3) of 3rd December 2020 completed on first half of 2022 (Gaia DR3). The photometric band of Gaia is in the visible and NIR up to 1μm, that means it can be suitable for NIR but requires photometric information from other catalogues for the Mid-Far IR. For this reason three other all sky catalogues have been considered: the near-infrared Two Micron All Sky Survey point source catalogue (2MASS) with magnitude on 3 IR bands J, H and Ks but with low astrometric accuracy; and the two releases of the Wide-field Infrared Survey Explorer mission (WISE [10]): the mid-infrared CatWISE2020 catalogue [reference XX], and the both mid- and far-infrared AllWISE catalogue. Because of the poor astrometric accuracy of these catalogues, a cross-match with Gaia sources is mandatory. A cross-match between CatWISE and Gaia performed by INAF shows about 50% of CatWISE sources matched, while the cross-match between AllWISE and Gaia DR2, done

as part Gaia project [11], shows about 300 000 AllWISE sources matched.

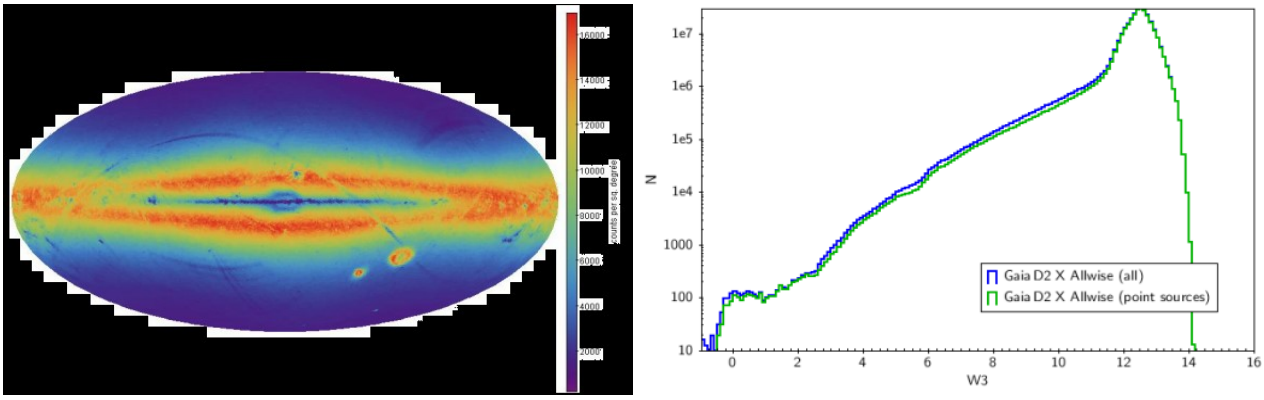

Figure 3. Sky map with counts per square degree of the AllWISE sources matched with Gaia DR2 (Left). Magnitude distribution of Gaia-AllWISE catalogue in W3 band (right).

The operative condition of the detector drives the choice for the accommodation. In fact the NIR detector can only be placed in the 30K environment outside the Focal Plane, while the Mid-Far IR detector shall be operated in the cryogenic environment inside the Focal Plane. The investigation of the accommodation based on preliminary configuration of SPICA Observatory for the two satellite system studies, concluded that there would be sufficient volume in the Focal Plane Instrument Assembly for the FGS channel optics, detector and readout electronics; the allocated field of view at focal plane level corresponds to 300"x300" and has been assessed sufficient for star coverage at North Galactic Pole (which in principle is the region with lower star density). Regarding alternative accommodation, none of the of the SPICA System studies showed possible allocation for FGS units outside Focal Plane Instrument Assembly (FPIA); for this reason, the accommodation and the FGS solution based on NIR detector has been discarded.

Since the Si:As detectors for MIRI instrument is discontinued, the only viable solution is an FGS in the Mid-Far IR based on the Si:As or Si:Sb detector from DRS accommodated inside the Focal Plane Instrument Assembly. Despite the results of the trade-off analysis, it has been communicated by ESA at the beginning of 2021 that a solution based on a separate equipment was no longer affordable and the FGS shall share the design of SMI/CAM instrument part of SPICA Observatory.

3 SPICA FGS BASELINE SOLUTION

The FGS baseline solution that has been studied, exploits the SMI/CAM design reported in Figure 4. The SMI/CAM channel passband and detector readout frequency would be adapted to cope with both scientific and guiding purposes, for this reason a passband centred at 28μm with 7μm width has been selected by ESA. The single SMI/CAM detector is based on Si:Sb technology and consists in four 512x512pixels independent quadrant in a square configuration resulting to 1024x1024 pixels array. The thermal, mechanical and electrical interfaces are guaranteed by the detector module which provides an environment with temperature below 2.0 K for Si:Sb detectors (and below 5.0 K for Si:As). In order to reduce the heat dissipation, a buffer amplifier is placed at an intermediate temperature stage (e.g., ~130 K) to transfer analogue signal to the warm electronics. The SMI/CAM optical channel foresees a FoV of 716"x600" imposed on a virtual 716"x716" FoV defined by the Si:Sb detector area. The plate scale is such that angular dimension of one pixel is 0.7 arcsec and most of the signal is contained inside a region of 6 pixel diameter.

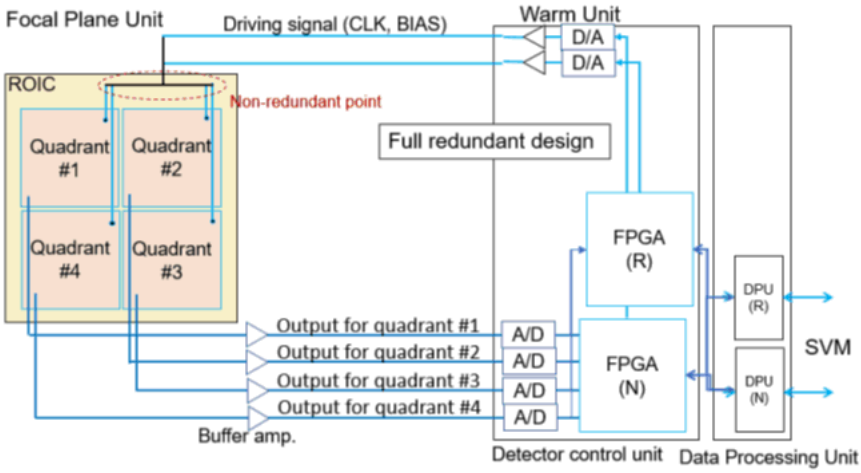

Figure 4. SMI/CAM design – baseline FGS solution for SPICA mission

The assessment of the performance started from the computation of the Signal-to-Noise for different integration time between 1 and 9 seconds. The collected signal is calculated through the reference Vega emission spectrum and the noise includes shot noise, sky background noise (zodiacal light and cirrus emission), straylight, detector noise (readout noise and dark current). The SNR has been evaluated for North Galactic Pole (NGP) and Galactic Center (GC) background conditions. The results are provided in terms of minimum detectable magnitude (magnitude at which central pixel saturates) and maximum detectable magnitude (magnitude at which SNR=5). With the selected telescope configuration and SMI/CAM channel properties, it is possible to detect up to mag 9 (which is the maximum in-band magnitude of the Gaia-CatWISE cross-matched star catalogue) with 7s at NGP, while at GC it shall be used a shorter integration time to detect non-saturated objects.

Table 2: Minimum and maximum detectable magnitude (at NGP and GC)

	Minimum magnitude SMI/CAM @28um		Maximum magnitude SMI/CAM @28um	
	NGP	GC	NGP	GC
T_exp = 1s	3.4	2.8	7.4	7.0
T_exp = 3s	4.7	4.3	8.5	7.7
T_exp = 5s	5.3	5.6	9.0	8.1
T_exp = 7s	5.6	11	9.25	8.3
T_exp = 9s	5.9	>11	9.45	8.4

As part of the study, Thales Alenia Space Italy developed a simulator able to import a Point Spread Function (PSF), adding all the noise contribution mentioned above and performing the estimation of the barycentre of the spot. This simulator has been used to evaluate the performance of the star centroid measurement through various simulations in which the centre of the PSF has been moved inside the pixel. The performance has been split in accuracy (the variable part of the error due to temporal and spatial effects) and in precision (the constant part of the error due mainly to the shape of the PSF considered). The simulation in the static case showed an accuracy of 20 mas, quite constant for all magnitudes, and a precision of 40 mas at 1 sigma (Figure 5). The simulation of PSF in movement with various angular rate showed a high degradation of the precision already at 2"/s leading to a limiting magnitude of 7.5mag and worst case precision of 0.4 arcsec at 1 sigma.

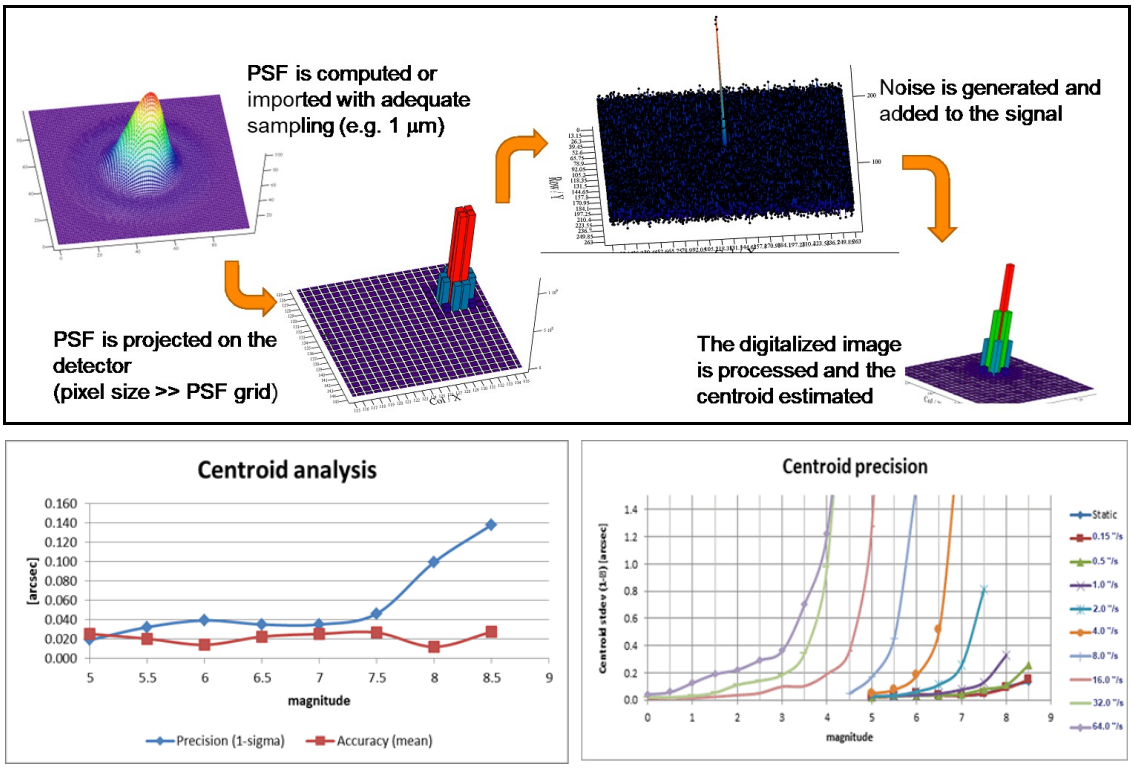

Figure 5. Steps of the PSF simulation and centroid computation (top). Centroid performance results for static PSF (bottom-left) and for dynamic PSF (bottom-right).

The exposure time to be used shall be selected in order to allow good detection of the stars present in the star catalogue. The investigation of available catalogues showed that there is not currently a star catalogue with the magnitude measured at 28µm wavelength; therefore it is required an important effort to propagate the photometry of catalogue object from the closest band, which is AllWISE catalogue W4 band at 22µm, to the actual band. With the aim to have a preliminary assessment of the FGS performance an extrapolation of W4 magnitude into 28µm band has been done based on BlackBody emission but it is remarked that this is not consistent with the emission spectrum of the sources with emission in the Far-IR (galaxies, QSO, stars surrounded by dust) and therefore there is no reliability on the derived magnitude.

The star catalogue coverage has been evaluated at North Galactic Pole (NGP), thanks to a test catalogue provided by INAF Astrophysical Observatory of Turin reporting J, W1, W3 and W4 magnitudes, and at small region close to Galactic Center (GC), where cumulative magnitude distribution in W4 band has been provided by ESA. After derivation of the magnitude in 28 µm band, the results is that at the NGP most of the catalogued objects are inside the range 5 – 9 mag, while at the GC are expected in 3 – 7 mag range. According to Table 2 the preferred solution is therefore to use different integration time depending on the sky region. In order to have margins (to cope with the uncertainty related to the magnitude extrapolation) the exposure time shall be 7s at NGP and 1s at GC. In case a common integration time is required for design limitation 5s would be a possible option but degrading coverage at GC and with no margin at NGP.

Assuming a homogeneous distribution of sources inside the NGP and GC region, the estimation of average number of stars in FoV is done based on the objects detectable with the selected integration time. Thanks to Poissonian statistics, it is then possible to derive the number of stars expected at 95% of confidence level. The results are provided in Table 3. The worst coverage at Galactic center shall not be a surprise. In fact on the Galactic plane there is an important increase of the sky background (Zodiacal light but in particular Cirrus emission) limiting the maximum detectable

magnitude, and the high number of stars increases the probability of neighbouring source merging. For a sensitivity on the FoV dimension it has been considered the case of 4 quadrant FoV (corresponding to 0.04 deg2) and the case of 3 quadrant FoV (corresponding to 0.03 deg^2).

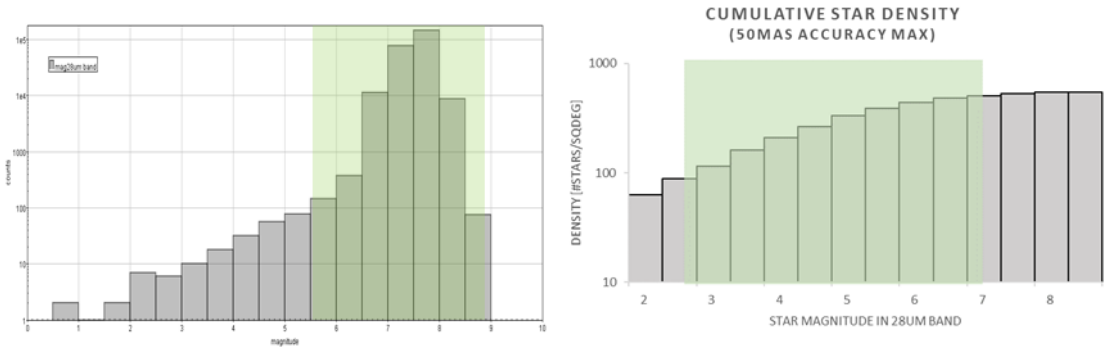

Figure 6. Differential magnitude distribution in 28μm band (logarithmic scale) at NGP (left) and cumulative at GC (right)

The information collected about the readout frequency of the Si:As and Si:Sb Readout Integrated Circuit (ROIC) fixes into 240 kpix/s per output the maximum rate, and having 4 output the full detector can be dumped in about 1s. Considering the maximum integration time of 7 seconds the worst case FGS sampling time is 8 seconds. This is in general terms quite high as attitude measurement sampling time, but it is the best possible with the assumed SMI/CAM design in FarIR region: the reduction of the integration time would have in fact significant impacts on the SNR and as a consequence on the sky coverage.

Table 3: Star coverage statistics at different FoV dimension

FoV dimension	Average number of star in FoV	Number of stars in FoV @ 95% of probability	% of sky region with ≥ 5 stars
4 quadrant @ NGP	68	> 30	> 99.7%
4 quadrant @ GC	15	8	99%
3 quadrant @ NGP	51	> 30	> 99.7%
3 quadrant @ GC	13	6	98%

3.1 SPICA FGS Performance

The Absolute Knowledge Error (AKE) is the instantaneous value of the knowledge error at any given time and, with reference to the attitude, is the difference between known (estimated) absolute attitude and the actual absolute attitude of the Observatory. The Absolute Knowledge Error is composed by several contributors according to [12]; the effect of these contributors can be summarized into 3 main categories: bias, field dependent bias and time random noise.

The Bias has been estimated considering the contribution of detector alignment knowledge (1μm in position and 10 arcsec in tilt) and the focal length knowledge (0.01% of overall focal length, i.e. considering both telescope and SMI/CAM channel optics).

The field dependent bias is the actual bias of one scientific scene and includes the contribution of the star catalogue accuracy (estimated in 25mas 1σ per axis) and the centroid measurement accuracy. In addition, it depends on the number of stars inside the FoV. The time random noise includes all the effects due to the detector response, signal readout and measurement algorithm which effect varies from one acquisition to the other; all these contributors are accounted into the centroid measurement precision reported previously that depends on the magnitude of the star and on the angular rate.

The field dependent bias and the time random noise, that does not linearly sum, have been estimated through Montecarlo simulation, where the dispersed parameter are the number, position and magnitude of the stars and the error contributor according to Gaussian statistics. The simulated number of stars reflects the statistics of NGP and GC coverage and the position of the stars on the detector is propagated based on the dynamic condition to have a realistic estimation of the AKE in low and high angular rate. The maximum angular rate considered for the simulation is 2"/s, being the one which is still assuring sufficient number of stars in FoV (maximum detectable magnitude is 7.5 mag). The AKE values refer to the results at Galactic Center for a FoV of 3 quadrant (worst case situation in terms of number of stars).

Table 4: Absolute Knowledge Error budget preliminary estimation

	X axis (arcsec)	Y axis (arcsec)	Z axis (arcsec)
Bias	0.043	0.071	6.288
Field dependent bias (low rate)	0.077	0.043	19.124
Field dependent bias (high rate)	0.376	0.133	110.508
Time random noise (low rate)	0.048	0.025	14.167
Time random noise (high rate)	0.546	0.201	159.899
Thermo-elastic distortion	TBD	TBD	TBD

The spacecraft thermo-elastic distortion, affecting the alignment of the FGS LoS with respect to the S/C axes has not been evaluated because requiring higher knowledge of the spacecraft configuration and thermal properties. It is reported only for completeness.
All the trade-off and analysis performed lead to a definition of a preliminary list of technical requirements applicable to the design of a Fine Guidance Sensor for the SPICA mission based on the SMI/CAM and to define a development plan to reach a target TRL 6 within 3-4 years.

4 FAR IR STAR CATALOGUE ANALYSIS

The analysis of the FGS architecture and trade-off for the SPICA baseline solution highlighted the complexity in generating a star catalogue for the Far-IR region by cross-matching Gaia catalogue for the astrometry with other IR catalogues for the photometry. The worst case coverage found at Galactic Centre is partially due this cross-match process. Furthermore the prediction of the photometry in a band that is not covered by all-sky and accurate catalogues can impact the real number of sources detectable by the FGS with consequence in the sky coverage and performance. With the aim to investigate further the feasibility of a Fine Guidance Sensor in the Far IR domain ESA founded a second study in 2022 with as objective:

- to characterize the detectable star density over an extended region around the Galactic Centre identifying the optimum FGS exposure time
- to analyse and to model the photometric transformations from AllWISE W3 &W4 bands to Far IR

The consolidation of the sky coverage in the Galactic Center is based on a star catalogue generated by TAS-I covering 10°x10° around the GC and reporting all the cross-matched sources between Gaia DR3 and AllWISE (the cross match is done by Gaia consortium and available on Gaia data website [11]).

The analysis of the cross-match method was focused in defining those characteristics that can provide good targets for Fine Guidance Sensor tracking in the infrared region. In this sense, to assure accurate astrometry, it is selected as candidate good targets all sources having 5 astrometric parameters, without "mates" (i.e. no other Gaia sources crossmatched with same AllWISE source), and with a distance between Gaia and AllWISE lower than 0.5 arcsec. The density of the candidate good targets in the vicinity of GC region shows a very good coverage for Galactic latitude from 1 deg up to 5 deg (region of Galactic Bulge with average density of 400 source/FoV) with a sudden decrease lower than 1 deg (down to 30-50 source/FoV) because the detection of the stars is affected by the high IR background and by the strong interstellar extinction.

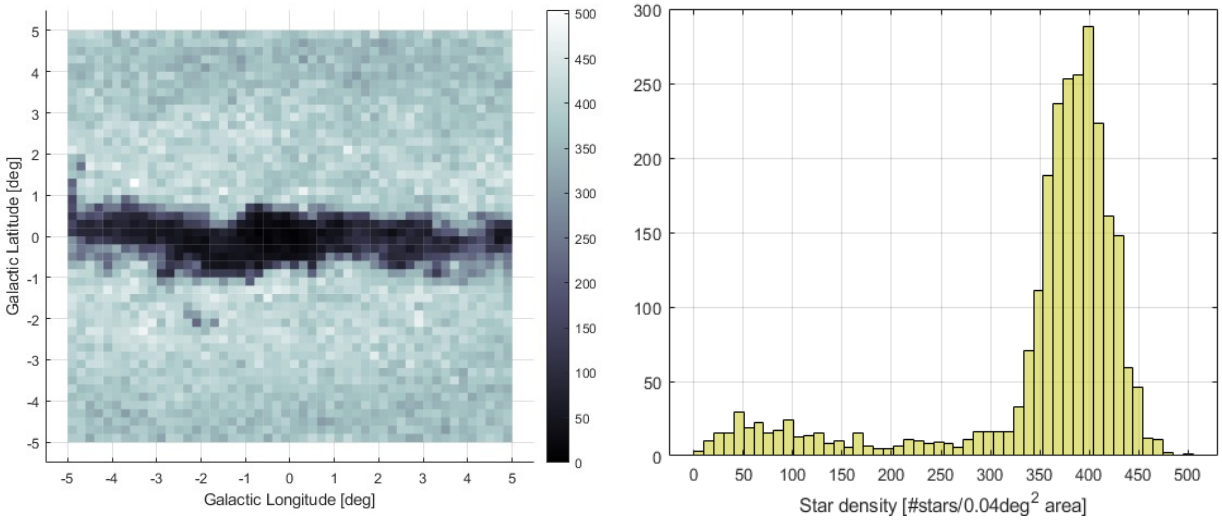

Figure 7. Source density map around GC (left). Colour scale identifies the number of sources inside a FoV of 0.2°x0.2°. Histogram of number of sources in FoV (right)

To assess the photometric propagation in the Far IR and the expected accuracy the INAF Astrophysical Observatory of Turin performed a cross-match between Gaia-AllWISE sources with with Spitzer MIPS catalogue ([13] and [14]) having photometry at [24]μm wavelength identifying 3607 sources in a 11.5 deg^2 region at intermediate Galactic latitude towards the South Ecliptic Pole (SEP). In addition 5398 Spitzer/MIPSGAL sources were cross-matched in a 3.14 deg2 region towards the GC.
The cross-match with IRAS ([15]) at [25]μm wavelength brought identification of 143 and 318 matched sources respectively at NGP (within 20°) and at GC (within 2°) very few and too bright to be used in view of FGS use.

In the field towards the South Ecliptic Pole, the AllWISE magnitudes W4 (centred at 22μm) has been compared with IRAS [25]μm and Spitzer/MIPS [24]μm. The first result is the confirmation that W4 ≈ [24]μm ≈ [25]μm due to the similarity of these three passbands. A pragmatic rule for source classification it is proposed, by means of the color-color plot G–W1 vs. W2–W3 to distinguish stars and extragalactic objects (see Figure 8). It is demonstrated that stars above the Galactic plane and without IR excess (i.e. stars not surrounded by dust and not affected by interstellar extinction) have null IR color-indexes in the standard Vegamag photometric system, so that W2 ≈ W3 ≈ W4 ≈ [24]μm, as the spectral energy distribution in the MIR and FIR can be well represented by the Rayleigh–Jeans approximation. Extragalactic sources show positive color-indexes of about W3–W4 ≈ 2.4 mag, due to the thermal emission from the dust in their Inter Stellar Medium.
The photometric propagation close to the Galactic Center is a much more challenging region because of the stellar crowding, as well as the strong optical extinction associated with a high sky IR background. The distribution [24]μm vs. W3 in the GC region shows a larger spread and

systematic offset with respect to the corresponding distribution in the SEP region (probably due to an instrumental systematic bias produced by the high sky background that contaminates the photometric aperture of the lower resolution WISE data).

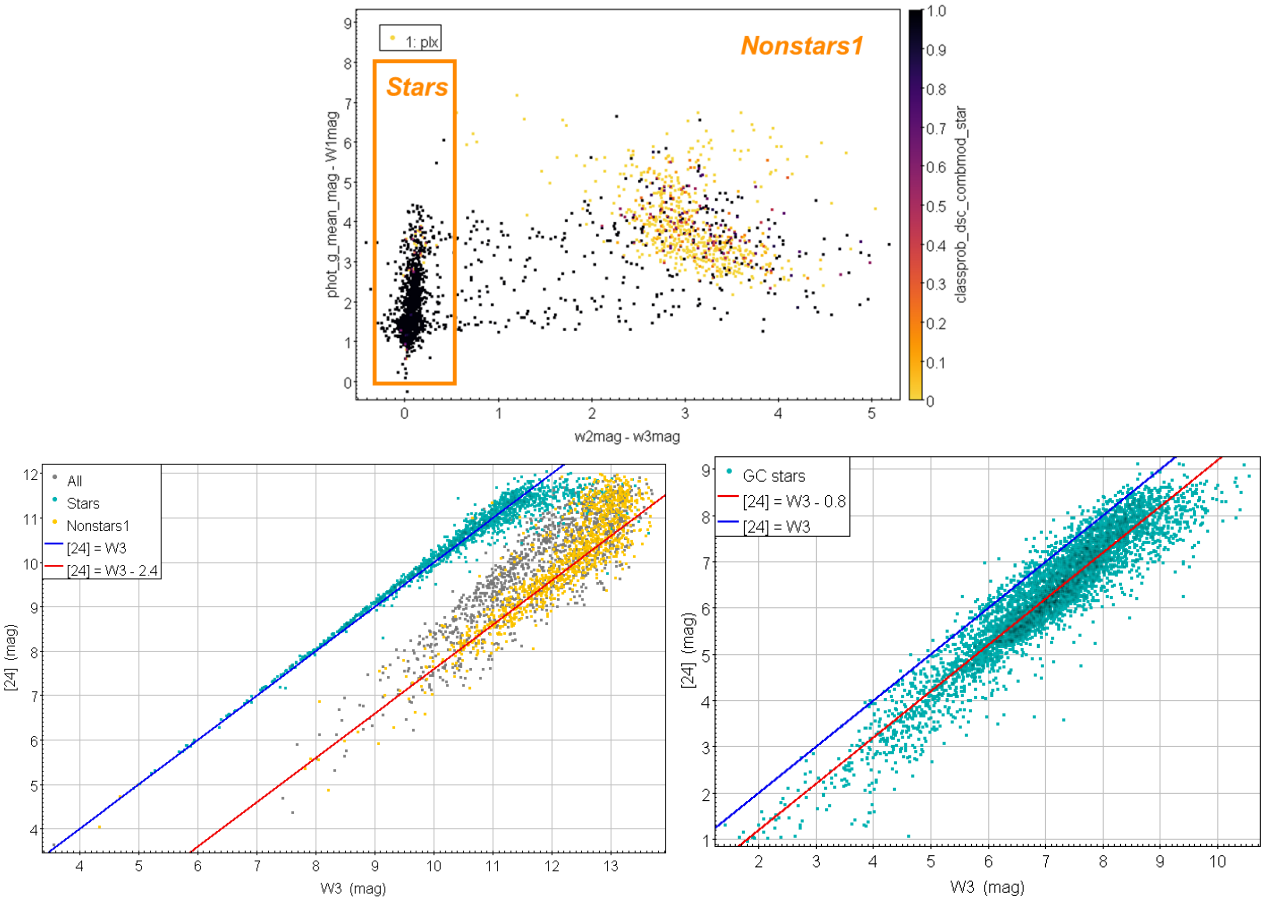

Figure 8. Source classification by INAF based on color-color rule (top). Photometric transformations from W3 to SPITZER [24]μm in the SEP field that can be adopted for the regions above the Galactic plane (bottom left). Nonstars1 are extended objects (Galaxies/QSO) with 5 astrometric parameters. Photometric transformation in the GC field that can be adopted for the regions close to the Galactic plane (bottom right).

INAF derived photometric transformations from W3 to the [24]μm passband for both the SEP and GC regions within the magnitude range defined by the sensitivity of AllWISE and Spitzer/MIPS surveys. The accuracy of these transformation in the SEP region increases from 0.04 mag ($W3 < 7$) to 0.18 mag ($W3 \approx 11$). For non-stellar sources with 5 astrometric parameters (Nonstars1 in Figure 8) the accuracy is about 0.3-0.5 mag in the range $8 < W3 < 14$.

The photometric transformation for the stellar sources in the GC field shows an offset of 0.8 mag offset with respect to the bisector [24] = W3 that evidences a systematic bias affecting AllWISE or Spitzer photometry, due to local high IR background. Such bias depends on both the technical features (e.g. resolution) of the instrument and on the implemented photometric reduction method (e.g. background estimation, PSF/aperture photometry, etc…); this fact could affect as well the photometry propagation for future IR missions depending on the design. The observed offset between AllWISE and Spitzer can vary in other Galactic plane regions with different IR sky background. The characterization of the bias would represent an important effort for building a star catalogue for a future Far IR FGS if requiring usage of W3 magnitude (or longer wavelegth).

Table 5: Photometric transformations defined in the SEP and GC fields that can be adopted respectively for the regions above the Galactic plane and close to Galactic plane

Objects	Transformation	Accuracy (mag)
SEP field		
Stars	**[24]μm = W3** valid for objects W3 < 11 AND [24] < 11	mean: -0.06 sigma: 0.14
Nonstars1	**[24]μm = W3 – 2.4** valid for objects W3 < 14 AND [24] < 11	mean: -0.04 sigma: 0.40
GC field		
Stars	**[24]μm = W3 – 0.8** valid for objects W3 < 11 AND [24] < 10	mean: +0.02 sigma: 0.47

Thanks to these outcomes it has been possible to upgrade the formula for determining the 28μm magnitude relying on Black Body emission used in the first performance assessment. The sky coverage at 28μm in the Galactic Center region has been re-evaluated by considering signal-to-noise of baseline solution (SMI/CAM) of previous SPICA FGS study to derive the source detected with three different exposure time: 1, 3 and 5 seconds.

The tradeoff on the best exposure time shows that 5 seconds is the best solution for the Galactic Center region and, considering sources from the cross-matched AllWISE–Gaia DR3 catalogue, there is 90% of probability in the 10°x10° region to have more than 30 sources/FoV that is the maximum number of sources planned to be used for attitude determination in flight. In the GC region only one critical field of view is observed with less than 5 stars. The result is much better than what was found as conclusion of SPICA FGS study for the GC field and with this sky coverage it is reasonable to expect the AKE performance derived for the NGP region with a useful area corresponding to 3 quadrants (Table 4).

With the updated photometric transformations, a quick assessment of the sky coverage at NGP has been repeated. Unexpectedly it is found that the W3 catalogue magnitude, used for propagation at 28um wavelength, is saturated for most of the objects and therefore there would be high uncertainty in the resulting magnitude. To be on the safe side, it can be considered only the sources with reliable W3 magnitude (W3<11.5) but the resulting coverage is too low for guaranteeing the FGS tracking. As conclusion it is found that despite some local worst case region very close to the GC exist, the NGP is still the worst case region in terms of density of detectable sources for an FGS in the Far-IR band if considering only objects with reliable W3 magnitude.

Table 6: Source density at GC and NGP in Average over 10°x10° and Worst Case density inside a square degree region

	Galactic Center (GC)	North Galactic Pole (NGP)
Cross matched catalogue density	**Average** = 14268 sources/deg^2 **WC region** = 2096 sources/deg^2	**Average** = 1758 sources/deg^2 **WC region** = 1439 sources/deg^2
Reliable and accurate catalogue density (Gaia-AllWISE angular distance < 0.5", single matches, W3 < 11.5)	**Average** = 6740 sources/deg^2 **WC region** = 1213 sources/deg^2	**Average** = 66 sources/deg^2 **WC region** = 44 sources/deg^2
Detectable source density (reliable and accurate sources detectable with the selected FGS exposure time)	*FGS exposure time 5 sec* **Average** = 1269 sources/deg^2 **WC region** = 395 sources/deg^2	*FGS exposure time 9 sec* **Average** = 27 sources/deg^2 **WC region** = 14 sources/deg^2

A summary of density statistics is provided in Table 6, where the density is given in sources/deg^2 to be more generic, while in previous section of the report is given sometimes as sources/FoV (FoV 0.2°x0.2°).

5 CONCLUSIONS

A significant number of analysis and trade-off has been carried out by TAS-I with the support of INAF to investigate the feasibility of a Fine Guidance Sensor at Infrared wavelengths. The preferred solution would be in the Near IR where consolidated detectors, readout electronics and star catalogue exist. In the case of SPICA mission, the system design would have required to exploit the Far IR that is more critical because of detector production discontinuity and most of all because of risks in the performance (both Sky coverage and attitude knowledge) driven by the star catalogue generation (cross-match needed between Gaia and AllWISE catalogues and photometry propagation to the FarIR). This last aspect has been deeply assessed with provision of photometric transformation from AllWISE W3 to SPITZER [24]μm magnitude assuring a good accuracy. The sky coverage in the Far IR confirms that the North Galactic Pole is still the most critical region in term of star coverage while at Galactic Center the low density is localized just in the proximity of the GC.

6 AKNOWLEDGEMENTS

For the opportunity to explore the feasibility of a Fine Guidance Sensor, TAS-I thanks ESA for founding and for tightly following the two studies (ESA Contract Nr. 4000129611/19/NL/GLC/vr for SPICA FGS feasibility assessment and 4000138516/22/NL/MGu for Far-IR FGS risk mitigation) whose results are reported in this paper. A special thanks to the team of INAF Astrophysical Observatory of Turin composed by A.Spagna, S. Perina and P. Re Fiorentin for the high quality of their work in the evaluation of existing IR star catalogues and for the photometric transformation assessment.

7 REFERENCES

[1] ESA-SPI-EST-MIS-RP-001, *SPICA Mission Study Summary Report*, 2021

[2] R.Blank, *THxRG Family of High Performance Image Sensors for Astronomy*, ASP Conference Series, Vol. 437

[3] Fielque, *Development of astronomy large focal plane array "ALFA" at Sofradir and CEA*, Proc. of SPIE 2018

[4] Love, *1024 x 1024 Si:As IBC detector arrays for JWST MIRI*, Proc. of SPIE 2005

[5] Ressler, *Performance of the JWST/MIRI Si:As detectors*, Proc. of SPIE 2008

[6] Mainzer, *Characterization of Flight Detector Arrays for the Wide-field Infrared Survey Explorer*, Proc. of SPIE 2008

[7] Khalap, *Antimony-doped silicon blocked impurity band (BIB) arrays for low flux applications*, Proc. of SPIE 2012

[8] Sakon, *Sensitivity Estimates for the SPICA Mid-Infrared Instrument (SMI)*, Proc. of SPIE 2016

[9] Kaneda et At, *SPICA mid-infrared instrument (SMI):conceptual design and feasibility studies*, SPIE 2018.

[10] Wright et al., *The Wide-field Infrared Survey Explorer (WISE): Mission Description and Initial On-orbit Performance*, AJ, 140, 1868 (2010)

[11] Marrese et al., *Gaia Data Release 2. Cross-match with external catalogues: algorithms and results*, A&A 621, A144 (2019)

[12] ECSS-E-ST-60-20C *Stars sensors terminology and performance specification*

[13] Gutermuth & Heyer, *A 24 μm Point Source Catalog of the Galactic Plane from Spitzer/MIPSGAL*, arXiv_1412.4751v1 (2014)

[14] Scott et al., *Spitzer MIPS 24 and 70 μm imaging near the South Ecliptic Pole: maps and sources catalogs*, ApJ SS, Vol. 191, p. 212 (2010)

[15] Knauer et al., *Analysis to stars common to IRAS and Hipparcos surveys*, ApJ, 552, 787 (2001)

[16] Eisenhardt et al., *The CatWISE Preliminary Catalog: Motions from WISE and NEOWISE Data, ApJ SS* 247, 69 (2020)